

Structure–Activity Relationships in 1,4-Benzodioxan-Related Compounds. 7.¹ Selectivity of 4-Phenylchroman Analogues for α_1 –Adrenoreceptor Subtypes

Wilma Quaglia,[†] Maria Pigni,[†] Alessandro Piergentili,[†] Mario Giannella,[†] Francesco Gentili,[†] Gabriella Marucci,[†] Antonio Carrieri,[‡] Angelo Carotti,[‡] Elena Poggesi,[§] Amedeo Leonardi,[§] and Carlo Melchiorre^{*||}

Department of Chemical Sciences, University of Camerino, Via S. Agostino 1, 62032 Camerino (MC), Italy, Pharmaco-Chemistry Department, University of Bari, Via E. Orabona 4, 70126 Bari, Italy, Research and Development Division, Recordati S.p.A., Via Civitali 1, 20148 Milano, Italy, and Department of Pharmaceutical Sciences, University of Bologna, Via Belmeloro 6, 40126 Bologna, Italy

Received October 19, 2001; Revised Manuscript Received January 17, 2002

WB4101 (**1**)-related compounds **5**–**10** were synthesized, and their biological profile at α_1 -adrenoreceptor (AR) subtypes and 5-HT_{1A} serotonergic receptors was assessed by binding assays in Chinese hamster ovary and HeLa cell membranes expressing the human cloned receptors. Moreover, their receptor selectivity was further determined in functional experiments in isolated rat prostate (α_{1A}), vas deferens (α_{1A}), aorta (α_{1D}), and spleen (α_{1B}). In functional assays, compound **5** was the most potent at α_{1D} -ARs with a reversed selectivity profile ($\alpha_{1D} > \alpha_{1A} > \alpha_{1B}$) relative to both prototype **1** and phendioxan (**2**) ($\alpha_{1A} > \alpha_{1D} > \alpha_{1B}$), whereas compound **8**, bearing a carbonyl moiety at position 1, was the most potent at α_{1A} -ARs with a selectivity profile similar to that of prototypes. The least potent of the series was the trans isomer **6**, suggesting that optimum α_1 -AR blocking activity in this series is associated with a cis relationship between the 2-side chain and the 4-phenyl ring rather than a trans relationship as previously observed for the 2-side chain and the 3-phenyl ring in **2** and related compounds. Binding affinity results were not in complete agreement with the selectivity profiles deriving from functional experiments. Although a firm explanation was not available, neutral and negative antagonism and receptor dimerization were considered as two possibilities to account for the difference between binding and functional affinities. Finally, compound **5** was selected for a modeling study in comparison with **1**, mephendioxan (**3**), and open phendioxan (**4**) to achieve information on the physicochemical interactions that account for its high affinity toward $\alpha_{1d/D}$ -ARs.

Introduction

All three subtypes ($\alpha_{1a/A}$, $\alpha_{1b/B}$, $\alpha_{1d/D}$)^{2–4} of the α_1 -adrenoreceptor (α_1 -AR) are members of the G protein-coupled receptor (GPCR) superfamily and are responsible for mediating the actions in the body of the neurotransmitter noradrenaline. Despite the widespread tissue distribution of these receptors and their involvement in a variety of physiological processes, the extremely high sequence homology in the classic ligand-binding domain across α_1 -AR subtypes has made it difficult to design therapeutic agents that can effectively target one receptor subtype while not affecting all others.⁵ Thus, there is an ongoing need for effective structure–activity studies based on selective ligands for α_1 -AR subtypes.

It has been claimed that α_{1A} -AR antagonists can be useful in the treatment of benign prostatic hyperplasia (BPH).⁶ As a matter of fact, in the human prostate, although mRNA levels are not necessarily in close correlation with the corresponding protein levels, mRNA for all three subtypes has been found with that for the α_{1a} subtype present in the greatest abundance.⁷ Re-

cently, it has been advanced that the α_{1B} -AR subtype may be involved in the regulation of blood pressure as α_{1b} knockout mice displayed a significantly reduced responsiveness to phenylephrine-induced increases in blood pressure.⁸ A potential therapeutic use for α_{1D} subtype antagonists has not been defined yet. However, it has been shown that the α_{1d} subtype is dominant in the human bladder detrusor.⁹ Furthermore, it seems that the α_{1D} receptor blockade may be of benefit for the irritative symptoms of BPH that result from involuntary contractions of the bladder smooth muscle.¹⁰ It derives that a valuable drug for the treatment of BPH symptoms would be one that would inhibit α_1 -ARs in the low urinary tract without blocking α_1 -ARs responsible for maintaining the vascular tone. Thus, a useful pharmacological agent might be an α_1 -AR antagonist, which is selective for the α_{1A} over the α_{1B} subtype and endowed also with activity at α_{1D} -ARs such as to provide some potential additional therapeutic benefit.¹¹

In continued efforts to identify potent and selective α_1 -AR antagonists, we have previously published on the structure–activity relationships leading to the design and synthesis of potent α_1 -antagonists whose chemical structure incorporated a 1,4-benzodioxan-2-yl or a closely related moiety as the main feature.¹² WB 4101 {*N*-[2-(2,6-dimethoxyphenoxy)ethyl]-2,3-dihydro-1,4-benzodioxin-2-methanamine, **1**, Figure 1} is the prototype of α_1 -AR antagonists bearing a benzodioxan moiety.¹³ Data

* To whom correspondence should be addressed. Tel.: +39-051-2099706. Fax: +39-051-2099734. E-mail: camelch@kaiser.alma.unibo.it.

[†] University of Camerino.

[‡] University of Bari.

[§] Recordati S.p.A.

^{||} University of Bologna.

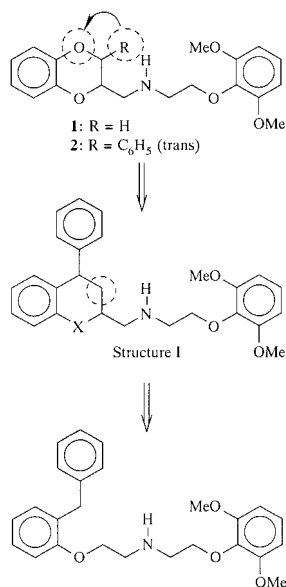
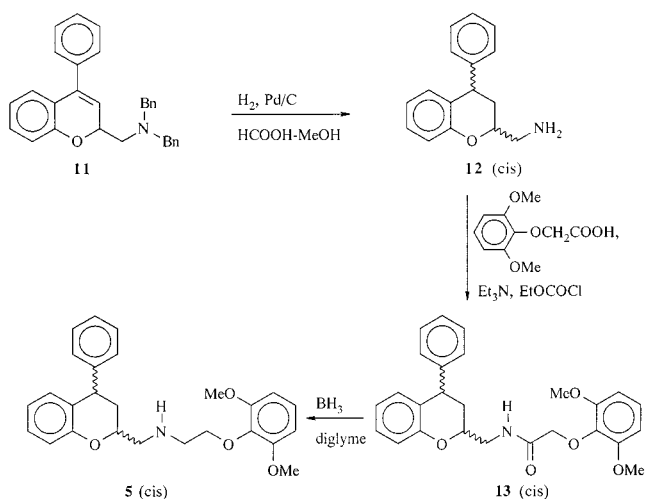


Figure 1. Design strategy for the synthesis of compounds 5–10 by changing the place of the phenyl ring from position 3 to 4 and replacing the oxygen atom at position 4 of **2** with a methylene unit and subsequent ring opening of structure I.

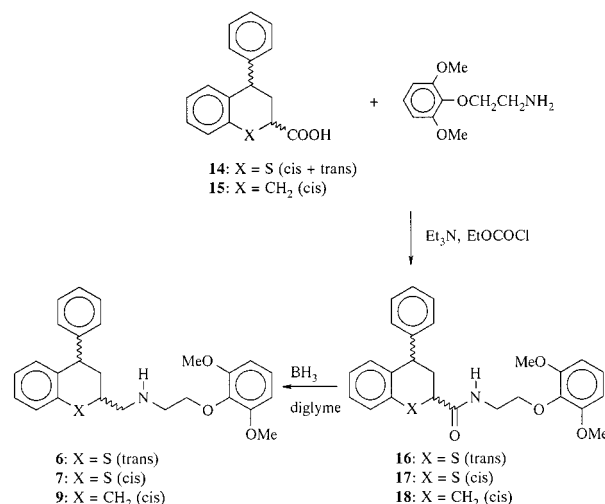
Scheme 1^a



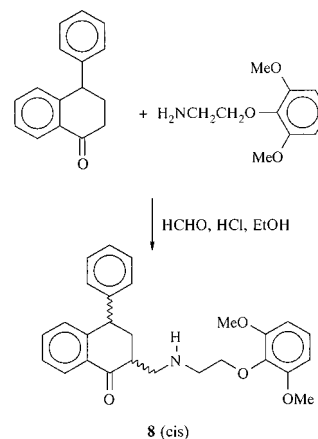
^a Bn = benzyl.

showed that the two oxygen atoms at positions 1 and 4 might have a different role in receptor binding.^{14,15} The oxygen atom at position 4 of **1** may play only a structural role as it could be replaced by a sulfur atom or a methylene unit without affecting potency toward rat vas deferens α_1 -ARs. On the contrary, the oxygen atom at position 1 of **1** appears to contribute to receptor binding because its replacement with a sulfur atom or a methylene group resulted in a significant decrease in potency, whereas its replacement by a carbonyl function did not modify the biological profile at rat vas deferens α_1 -ARs. Among the many other structural modifications performed on **1**, the insertion of a phenyl ring or a *p*-tolyl moiety at the 3-position having a trans relationship with the 2-side chain afforded phendioxan {*trans-N*-[2-(2,6-dimethoxyphenoxy)ethyl]-2,3-dihydro-3-phenyl-1,4-benzodioxin-2-methanamine, **2**, Figure 1} or its *p*-tolyl analogue mephendioxan (**3**, Table 4), respectively, that displayed the highest affinity for native α_{1A} -ARs relative to both α_{1B} and α_{1D} subtypes.^{12,16} Interestingly, an open

Scheme 2



Scheme 3

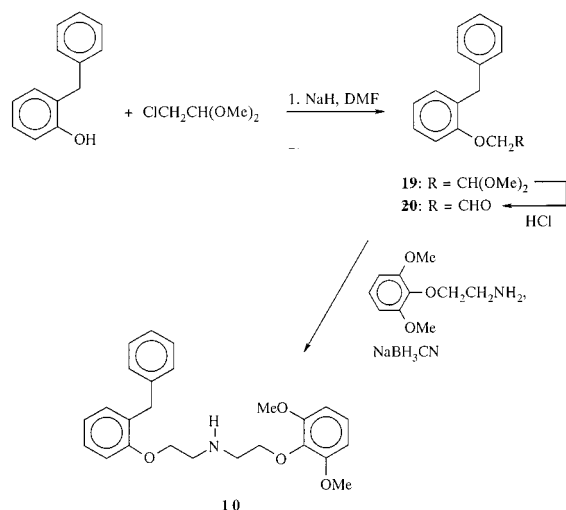


analogue of **2**, namely, **4** (Table 4), retained high affinity for α_1 -AR subtypes. However, contrary to **2**, compound **4** was more potent at $\alpha_{1D/D}$ -ARs than at both $\alpha_{1A/A}$ and $\alpha_{1B/B}$ subtypes.¹²

The present article expands on the study of another aspect of structure–activity relationships of **1**, namely, the effect of exchanging the oxygen atom at position 4 for a phenylmethine group, affording **5**. In turn, compound **5** has been modified by replacing the oxygen atom at position 1 with a sulfur atom, a carbonyl group, or a methylene unit, giving **6** and **7**, **8**, and **9**, respectively. Finally, the effect of opening the dihydropyran ring of **5** has been investigated by synthesizing compound **10**. The design strategy for these compounds is shown in Figure 1.

We describe here the synthesis of compounds 5–10 (Schemes 1–4) and the results of their screening at human cloned α_1 -ARs, expressed in Chinese hamster ovary (CHO) cells, and native α_1 -ARs in rat prostate, prostatic vas deferens, thoracic aorta, and spleen. Furthermore, to improve our knowledge on the main physicochemical interactions governing the ligand binding to the α_{1D} -ARs and to interpret at the 3D level the structure–affinity relationships of the adrenergic ligands reported in this paper, a series of docking experiments were undertaken with compounds 3–5 and **1**, the latter being taken as the reference ligand. Compounds **1**, **3**, and **5** differ in the presence and position of a phenyl

Scheme 4



substituent on the benzo-fused heterocyclic ring, whereas **4** can be considered an open analogue of **3**. The diverse activity profiles of these ligands might therefore be attributed either to a different binding mode or, most likely, to some favorable/unfavorable hydrophobic/steric interactions driven by the presence and spatial arrangement of the aryl group on the benzo-fused heterocyclic ring.

Chemistry

The compounds used in the present investigation were synthesized by standard procedures and characterized by ¹H nuclear magnetic resonance (NMR) and elemental analysis. Compound **5** was synthesized starting from **11**¹⁷ as shown in Scheme 1. Although amine **12** has been already reported,¹⁷ it was synthesized by following a different procedure through the catalytic hydrogenation of **11**. This reaction afforded only one of the two possible stereoisomers. (2,6-Dimethoxy-phenoxy)acetic acid,¹⁸ in chloroform, was amidated in the presence of Et₃N and EtOCOCl with amine **12** to give the corresponding amide **13**. The stereochemical relationship between the 2-side chain and the 4-substituent in **13** was determined by 1D nuclear Overhauser effect (1D NOE) measurements. A *cis* relationship between C₂-H and C₄-H of **13** was deduced by the observation that irradiation of C₄-H caused NOE at C₂-H (2%) and C₃-Ha (3%) and irradiation of C₂-H gave the same effect at C₃-Ha (2.5%). Reduction of **13** with borane–methyl sulfide complex in dry diglyme gave the corresponding amine **5**.

Isomers **6** and **7** and the carbon analogue **9** were synthesized as shown in Scheme 2. Basic hydrolysis of a mixture of *cis*- and *trans*-4-phenyl-thiochroman-2-carboxylic acid ethyl ester¹⁹ afforded a *cis/trans* mixture (ratio 1:1) of the corresponding acid **14**. Acids **14** and **15**,²⁰ in chloroform, were amidated in the presence of Et₃N and EtOCOCl with 2-(2,6-dimethoxy-phenoxy)-ethylamine²¹ to the corresponding amides **16**–**18**. Isomers **16** and **17** were separated by column chromatography. Reduction of amides **16**–**18** with borane–methyl sulfide complex in dry diglyme gave the corresponding amines **6**, **7**, and **9**. The stereochemical relationship between the amino side chain and the phenyl ring in **6** and **7** was determined by 1D NOE measurements. In

compound **6**, the C₄-H at δ 4.33 ppm is equatorial (*J* = 2.3 Hz). The irradiation of C₄-H caused no NOE effect at C₂-H. However, because of the C₃-H multiplicity, it can be deduced that C₂-H is axial and therefore *trans* to C₄-H. In compound **7**, the irradiation of C₄-H caused NOE effect at C₂-H. Moreover, C₃-H_a at δ 2.02 ppm coupled with three protons with high coupling constants (*J* = 10.5, 12.3, 13.3 Hz), indicating that C₂-H and C₄-H are axial and therefore *cis*. Consequently, the stereochemical relationship between the 2-side chain and the 4-substituent is *trans* in **6** and *cis* in **7**.

Compound **8** was synthesized by a Mannich reaction of 4-phenyl-1-tetralone²² and 2-(2,6-dimethoxy-phenoxy)-ethylamine²¹ and paraformaldehyde (Scheme 3). This reaction afforded only one of the two possible isomers. The stereochemical relationship between the 2-side chain and the 4-substituent in **8** was determined by 2D NOE (nuclear Overhauser enhancement spectroscopy) measurements. Compound **8** showed cross-peaks between C₄-H and C₂-H; moreover, both C₄-H and C₂-H showed cross-peaks with the same C₃-H_a, indicating a *cis* relationship between C₂-H and C₄-H.

Open analogue **10** of **5** was synthesized as shown in Scheme 4. Alkylation of 2-benzyl-phenol with chloroacetaldehyde dimethyl acetal gave **19**, which, in turn, was transformed into the aldehyde **20** by acidic hydrolysis. Reductive amination of **20** with 2-(2,6-dimethoxy-phenoxy)ethylamine²¹ gave **10**.

Biology

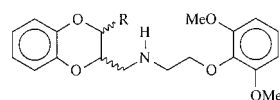
Binding Experiments. The pharmacological profile of compounds **5**–**10** was evaluated by radio-receptor binding assays using **1** and 8-[2-[4-(2-methoxyphenyl)-1-piperazinyl]ethyl]-8-azaspiro[4.5]decane-7,9-dione (BMY-7378) as standard compounds. [³H]Prazosin was used to label cloned human α₁-ARs expressed in CHO cells.²³ Furthermore, [³H]8-hydroxy-2-(di-*n*-propylamino)tetralin was used to label cloned human 5-HT_{1A} receptors expressed in HeLa cells.^{24,25}

Functional Studies. Receptor subtype selectivity of compounds **5**–**10** was further determined at α₁-ARs on different isolated tissues using **1**, **2**, and BMY-7378 as standard compounds. α₁-AR subtypes blocking activity was assessed by antagonism of (–)-noradrenaline-induced contraction of prostate²⁶ and prostatic vas deferens (α_{1A})²⁷ or thoracic aorta (α_{1D})^{28a} and by antagonism of (–)-phenylephrine-induced contraction of rat spleen (α_{1B}).^{28b}

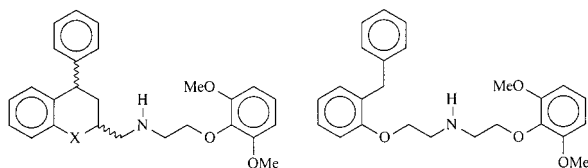
Results and Discussion

The functional activity, expressed as pA₂ or pK_B values, at α₁-AR subtypes of compounds used in the present study is shown in Table 1 in comparison with that of prototypes **1** and **2** and the reference compound BMY-7378, a selective α_{1D}-AR antagonist.

Analysis of the results reveals that all of the compounds were effective antagonists at α₁-ARs. Furthermore, all of the compounds were competitive antagonists at α₁-AR subtypes with the exception of **6**, **9**, and **10** at rat vas deferens α_{1A}-ARs and **6** and **10** at α_{1B}-ARs for which a Schild analysis could not be performed due to a depression of the maximal response to the agonist by antagonist concentrations higher than 1 μM. Interestingly, the antagonist affinities calculated in rat prostate

Table 1. Antagonist Affinities, Expressed as pA_2 Values, of **1**, **2**, **5–10**, and BMY-7378 at α_1 -ARs on Isolated Rat Prostate, Prostatic Vas Deferens (α_{1A}), Thoracic Aorta (α_{1D}), and Spleen (α_{1B})^a

1: R = H
2: R = Ph (trans)



5: X = O (cis)
6: X = S, (trans)
7: X = S (cis)
8: X = CO (cis)
9: X = CH₂ (cis)

10

compd	pA_2			
	prostate (α_{1A})	vas deferens (α_{1A})	spleen (α_{1B})	thoracic aorta (α_{1D})
1	9.27 ± 0.07	9.51 ± 0.06	8.16 ± 0.09	8.80 ± 0.12
2	8.23 ± 0.09 ^c	8.24 ± 0.07	5.60 ± 0.08	7.49 ± 0.06
5	8.95 ± 0.07 ^c	8.88 ± 0.02	7.54 ± 0.01	9.56 ± 0.09
6	6.97 ± 0.05 ^c	6.68 ± 0.10 ^b	6.52 ± 0.14 ^b	7.21 ± 0.09
7	8.31 ± 0.22 ^c	8.21 ± 0.06	6.81 ± 0.03	7.76 ± 0.02
8	9.46 ± 0.05 ^c	9.35 ± 0.08	7.58 ± 0.19	8.70 ± 0.09
9	6.54 ± 0.10	6.75 ± 0.10 ^b	6.96 ± 0.06 ^b	7.04 ± 0.01
10	7.47 ± 0.20	7.23 ± 0.09 ^b	7.17 ± 0.01	7.78 ± 0.08
BMY-7378		7.01 ± 0.08	7.48 ± 0.09	8.40 ± 0.09

^a pA_2 values ± SE were calculated according to Arunlakshana and Schild^{51a} unless otherwise specified, constraining the slope to -1 .^{51b} pA_2 is defined as the negative logarithm to the base 10 of that dose of antagonist that requires a doubling of the agonist dose to compensate for the action of the antagonist. ^b The antagonist affinity was calculated from only one concentration because there was a depression of the maximum response to the agonist, which increased with increasing the antagonist concentration. ^c pK_B values were calculated according to van Rossum^{51c} in the range of 0.01–1 μ M.

and prostatic vas deferens did not differ to each other, confirming that each of these preparations can be used to study the α_{1A} -AR subtype.²⁶

It is clear that potency at α_1 -AR subtypes was definitely dependent on the stereochemistry and substitution pattern of the compounds. It turned out that contrary to the trans stereochemical relationship between the 2-side chain and the 3-phenyl ring observed for prototype **2** and related compounds,¹⁶ a trans relationship between the 2-side chain and the 4-phenyl group is not optimal for binding at α_1 -ARs as revealed by a comparison between the trans and the cis isomers **6** and **7**. Isomer **7** was significantly more potent (22–34-fold) than the trans isomer **6** at α_{1A} -ARs, while it was, however, only slightly more potent at both α_{1B} - and α_{1D} -ARs.

The role of the sulfur atom at position 1 in **7** was investigated by its replacement with an oxygen atom (**5**), a carbonyl group (**8**), and a methylene unit (**9**), while a cis relationship between the side chain and the phenyl ring was kept constant. It turned out that **5** and **8** were more potent than **7** at all α_1 -ARs, whereas the carbon analogue **9** was the least potent. This result confirms

Table 2. Affinity Constants, Expressed as pK_i , of Compounds **1**, **5–10**, and BMY-7378 for Human Recombinant α_1 -AR Subtypes and 5-HT_{1A} Receptors^a

compd	pK_i , human cloned receptors			
	α_{1A}	α_{1B}	α_{1D}	5-HT _{1A}
1	9.37	8.0	9.29	8.68
5	10.30	10.40	10.05	8.19
6	8.63	7.56	7.64	7.99
7	10.05	8.94	9.36	7.82
8	9.60	8.91	9.74	7.96
9	9.29	7.91	7.77	8.20
10	9.40	8.55	8.44	7.97
BMY-7378	6.42	6.15	8.89	9.43

^a Equilibrium dissociation constants (K_i) were derived from IC₅₀ values using the Cheng–Prusoff equation.⁵³ The affinity estimates were derived from displacement of [³H]prazosin and [³H]-8-hydroxy-2-(di-*n*-propylamino)tetralin binding for α_1 -ARs and 5-HT_{1A} receptors, respectively. Each experiment was performed in triplicate. K_i values were from two to three experiments, which agreed within ±20%.

the previous observation that the oxygen atom at position 1 of **1** may have a role in receptor binding.^{14,15} Interestingly enough, the oxo analogue **5** was more potent than prototype **2** at all α_1 -AR subtypes. Furthermore, it displayed a reversed selectivity profile relative to **2** ($\alpha_{1D} > \alpha_{1A} > \alpha_{1B}$ vs $\alpha_{1A} > \alpha_{1D} > \alpha_{1B}$). Compound **5** was even more selective than BMY-7378 for α_{1D} -ARs relative to α_{1B} -ARs, while it was, however, less selective relative to α_{1A} -ARs. On the other hand, the sulfur analogue **7** and the oxo analogue **8** behaved like prototype **2** as they were more potent at α_{1A} -ARs and less potent at α_{1B} -ARs with a similar selectivity profile, that is, $\alpha_{1A} > \alpha_{1D} > \alpha_{1B}$. It derives that from a functional point of view these new compounds may have a potential in the treatment of BPH. Opening the dihydropyran ring of **5** gave **10**, which turned out to be a much weaker antagonist than **5** at all α_1 -ARs.

The binding affinities, expressed as pK_i values, in CHO cells expressing human cloned α_1 -ARs and HeLa cells expressing human 5-HT_{1A} receptors of compounds **5–10** are shown in Table 2 in comparison with those of **1** and BMY-7378. Compounds **5–10** were investigated at 5-HT_{1A} serotonergic receptors because it is known that **1** and related compounds are effective ligands also for the 5-HT_{1A} receptor.¹² It turned out that all of the compounds were potent ligands toward 5-HT_{1A} receptors but their affinity was much lower than that of prototypes **1** and BMY-7378. Analysis of the results reveals that α_1 binding affinities of compounds **5–10** did not correlate with potencies observed in functional assays. It can be seen that while binding affinities of reference compound **1** are qualitatively and quantitatively comparable with pA_2 or pK_B values derived from functional experiments, those observed for **5–10** are not in agreement from both a qualitative and a quantitative point of view with functional affinities as shown in Table 3. It would suffice to note that the carbon analogue **9** was a markedly weaker antagonist than **5**, **7**, and **8** at α_{1A} -ARs in functional experiments, whereas it displayed high affinity in binding assays, resulting in a selective α_{1A} antagonist ($\alpha_{1A} > \alpha_{1B} = \alpha_{1D}$). Furthermore, the open analogue **10**, which was a weak antagonist in functional experiments, was potent in binding assays with an affinity almost comparable to that of prototype **1**. However, one aspect was confirmed by binding experiments, namely, that a cis stereochemical relationship

Table 3. Differences in Antagonist Potency between Functional and Radioligand Binding Assays^a

compd	$\alpha_{1a}/\alpha_{1A}^b$	α_{1b}/α_{1B}	α_{1d}/α_{1D}
1	1	1	3
5	24	724	3
6	64	11	3
7	62	135	40
8	1.5	21	11
9	142	9	5
10	112	24	5
BMY-7378	0.25	0.05	3

^a Differences in potency were calculated as the antilog of the difference between pK_i values at cloned receptors and pA_2 values at the corresponding native receptors from data reported in Tables 1 and 2. ^b pA_2 values for native α_{1A} receptors were the mean between the values obtained in prostate and the values obtained in vas deferens preparations.

between the 2-side chain and the 4-phenyl ring is optimal for interaction with α_1 -ARs. As a matter of fact, trans isomer **6** was consistently less potent than cis isomer **7** at all α_1 -AR subtypes.

Recently,²⁹ we discussed the possibility that if an antagonist does not adhere perfectly to the concept of neutral antagonism in the interaction with the receptor but behaves as an inverse agonist, then a discrepancy between affinity values estimated in functional assays and affinity values estimated in binding experiments may not represent a surprise, because the estimated affinities of inverse agonists are system-dependent. Interestingly, the prototype of the present study, WB 4101 (**1**), was shown to be an inverse agonist in a vascular model containing α_{1D} -ARs and a native and constitutively activated mutant of the α_{1a} subtype.³⁰ Thus, the 3-fold difference observed for **1** between binding and functional affinity at $\alpha_{1d/D}$ -ARs might be explained by the fact that **1** is an inverse agonist at this subtype, and as a consequence, its affinity is not system-independent. It is tempting to assume that a similar explanation might apply for the discrepancy observed between binding and functional affinities for the other compounds of the present investigation. However, other possibilities may offer themselves to rationalize the discrepancy between binding and functional affinities.

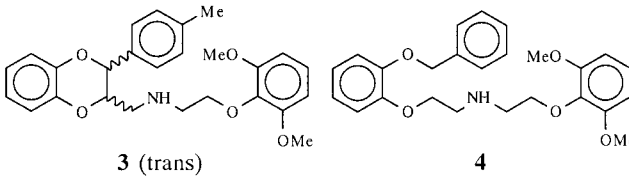
It has been generally assumed that GPCRs exist as monomers and couple to G proteins in a 1:1 stoichiometric ratio. However, increasing evidence indicates that such classical models of coupling between receptors and G proteins may be oversimplified.³¹ An increasing number of reports have described that receptor systems form dimers. It has been shown that dimerization of the receptor can occur when receptors are expressed in artificial systems and studies with chimeras have elucidated what part of the receptors participate in this interaction.³² However, it is clear now that dimerization and heterodimerization also occur in natural systems. It has been demonstrated that the GABA_BR1 and GABA_BR2 receptor subtypes form heterodimers in vivo that are required for proper cell surface receptor localization and function.³³ Furthermore, in another study,³⁴ it has been shown that κ and δ opioid receptors can form heterodimers with distinct ligand binding and functional properties, raising the possibility that heterodimerization may represent a more general mechanism to modulate GPCRs function. These observations of dimerization and, what may be even more intriguing, heterodimerization open a whole vista of possibilities for subtle

changes in the pharmacology of GPCRs, which may be due to dimerized receptors. These new receptor entities may not always signal as either a monomer or as dimers. It derives that the presence of homodimeric or heterodimeric receptors may certainly have profound ramifications with regard to the interpretation of biological data and, as a consequence, to the validity of structure–activity relationships. Thus, the discrepancy often observed, like in present case, between functional and binding affinities may not represent an anomaly because in screening procedures a homogeneous population of cloned receptors is used, which can be organized differently than native receptors in functional tissues and, consequently, their biological behavior may not be coincident. However, the discrepancy between functional and binding affinities observed in the present study may simply be accounted for by a different bioavailability of the compounds at the receptor level.

Notwithstanding, the discrepancy between functional and binding affinities, a molecular modeling study, was undertaken with compound **5** to get information on its mode of interaction with the α_{1d} -AR, using compounds **1**, **3**, and **4** for comparison. The choice of **5** was dictated by its very high affinity for both native and cloned $\alpha_{1d/D}$ -ARs.

The rhodopsin projection map^{35,36} has been extensively used as a major template to building 3D theoretical models of the seven transmembrane helices of GPCRs, by means of homology building approaches.³⁷ Very recently, a 2.8 Å resolution structure of the rhodopsin receptor, comprising extra- and intracellular loops, has been published.^{38,39} These structural investigations, along with site-directed mutagenesis studies,⁴⁰ have been extremely important to elucidate the complex binding and activation processes of diverse classes of GPCRs.⁴¹ A significant contribution to this field came just this year with the publication from some of us of a modeling study of the rat α_{1d} -AR.⁴² Such a study led to the identification of two distinct structural arrangements, corresponding to the resting and activated state of the receptor, and to the determination of the main structural requirements for an efficient binding to α_{1d} -ARs of both agonist and antagonist ligands.⁴²

Although the number of analyzed ligands is too low to derive any significant regression equation between measured binding affinities and estimated binding energies, relevant insights from this study might be gained, at a more qualitative level, by carefully analyzing and comparing the two data sets. The binding energies calculated for the docked ligands are reported in Table 4 along with their pK_i values. As it can be seen from Table 4, we were able to rank satisfactorily the pK_i data of most of the docked compounds in terms of estimated binding energies. The most active compound **4** shows a binding energy nearly three times lower than the least active compound **3** (−11.14 vs −3.35 kcal/mol), and also, compound **1** was adequately scored with respect to its pK_i values (−7.63 kcal/mol). In contrast, compound **5**, which has an activity close to that of compound **4**, showed a higher than expected binding energy (−7.44 kcal/mol). It is worth noting that the QXP package uses, “by definition”, a quick way to calculate interaction energy; therefore, it suffers from some limitations such as an insufficient parametrization of

Table 4. Affinity Constants (pK_i) and Binding Energies (kcal/mol) of Compounds **1** and **3–5**


compd	pK_i , human cloned α_{1d}	binding energy (QXP)	binding energy (GRID)
1	9.29	-7.63	-11.82
3	7.93 ^a	-3.35	-6.39
4	10.17 ^b	-11.14	-12.40
5	10.05	-7.44	-13.78

^a Data from ref 16c. ^b Data from ref 12.

the hydrophobicity for which no entropic effect is taken into account. This limitation can be overcome by estimating the binding energy with the latest version of the well-known GRID software.⁴³ Besides a well-parametrized force field for the calculation of the enthalpic contribution, in this method, the entropic component is also taken into account by considering the role of water in the solvation–desolvation phases of the binding process. Moreover, the calculation of the binding energy is carried out not only as the summation of the energetic contribution of the different atoms in the molecule considered as probe atoms but also considering the whole molecule as a probe.⁴⁴ So, we decided to apply this approach to recalculate the binding energies on the same receptor–ligand complexes retrieved by the QXP docking runs. As expected, the new values, reported in the last column of Table 4, show a good linear relationship with the pK_i values.

As can be seen from the molecular complexes in Figure 2, all of the compounds dock into the receptor binding site with a similar topology. In particular, the benzo-fused heterocyclic systems as well as the dimethoxyphenoxy group bind in a similar fashion. Some differences may be noted in the docked receptor–ligand **4** complex (see Figure 2D) where the benzyloxy moiety is much more buried into the core of the receptor helices bundle than that observed in complexes with ligands **3** (Figure 2B) and **5** (Figure 2C). Stronger favorable hydrophobic interactions can be therefore expected for compound **4**, and that was the case. It must be pointed out that this binding conformation can be attained only by ligand **4** because of its higher flexibility, as compared to the other ligands, all containing a benzo-fused, more rigid heterocyclic ring. The least active compound **3** places its *p*-tolyl substituent in a completely different, but easily accessible, receptor binding site (see Figure 2B). Its low pK_i value can be therefore ascribed to the lack of efficient hydrophobic contacts with the receptor counterpart. Moreover, with respect to the other ligands, compound **3** gives a poorer π – π aromatic stacking of the benzodioxan moiety with the phenyl ring of Phe358, which has been shown to play an important role in the binding of adrenergic ligands.⁴⁵

Finally, it is worth noting that in all of the four docked ligands of Figure 2, the common dimethoxyphenoxy moiety is always located closely to the charged nitrogen of Lys379 making possible the formation of a strong $N^+H\cdots O$ hydrogen bond between the positively charged

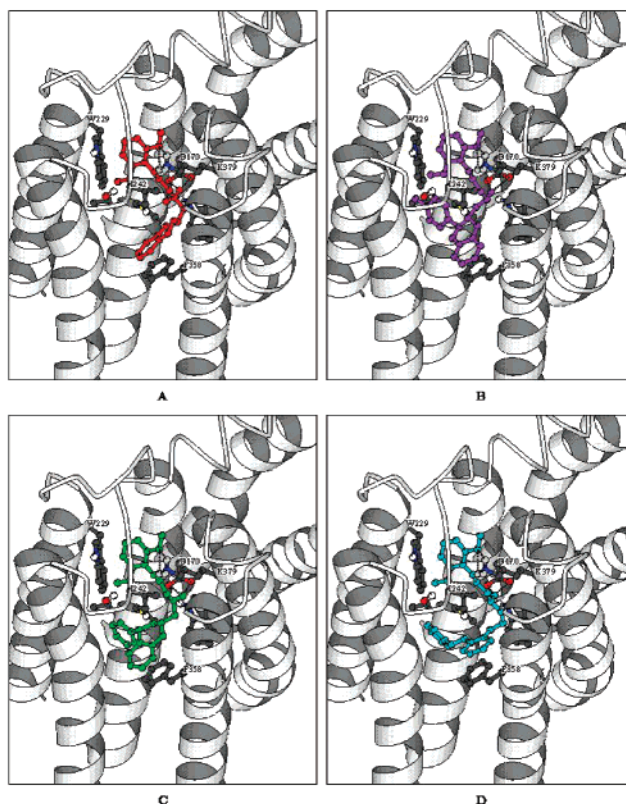


Figure 2. Compounds **1** (upper left red), **3** (upper right violet), **5** (lower left green), and **4** (lower right cyan) docked into the rat α_{1d} -AR binding site.

amine function of Lys and the oxygen atom of one methoxy group. At the same time, an edge-to-face π – π interaction between the dimethoxyphenoxy group and the Trp229 seems to take place.

Conclusions

A most intriguing finding of the present investigation was the observation that changing place to the phenyl ring from position 3, as in **2** and **3**, to position 4 caused, as far as α_1 -blocking activity is concerned, an inversion of the stereochemical relationship between the side chain and the phenyl ring. In fact, *cis* isomer **7** was significantly more potent than *trans* isomer **6** at all α_1 -AR subtypes, suggesting that optimal activity is likely associated with a *cis* relationship rather than a *trans* relationship as observed for **2** and analogues. Replacing the sulfur atom at position 1 in **7** with an oxygen atom (**5**) or a carbonyl function (**8**) improved markedly the affinity toward all α_1 -AR subtypes, whereas the replacement with a methylene unit (**9**) gave a significant decrease in affinity. These results parallel those obtained following the same structural modifications on **2**.¹⁶ In functional experiments, compound **5** was a potent and selective antagonist at α_{1D} -ARs relative to α_{1B} -ARs. Although the same selectivity profile was not observed in binding assays, compound **5** may be a useful lead for the design of more selective ligands for α_{1D} -ARs.

Experimental Section

Chemistry. Melting points were taken in glass capillary tubes on a Büchi SMP-20 apparatus and are uncorrected. IR and ¹H NMR spectra were recorded on Perkin-Elmer 297 and Varian VXR 300 instruments, respectively. Chemical shifts are reported in parts per million (ppm) relative to tetramethyl-

silane (TMS), and spin multiplicities are given as s (singlet), br s (broad singlet), d (doublet), dd (double doublet), ddd (doublet of double doublet), t (triplet), br t (broad triplet), dt (double triplet), q (quartet), or m (multiplet). Although the IR spectra data are not included (because of the lack of unusual features), they were obtained for all compounds reported and were consistent with the assigned structures. The elemental compositions of the compounds agreed to within $\pm 0.4\%$ of the calculated value. When the elemental analysis was not included, crude compounds were used in the next step without further purification. Chromatographic separations were performed on silica gel columns (Kieselgel 40, 0.040–0.063 mm, Merck) by flash chromatography. The term "dried" refers to the use of anhydrous sodium sulfate. Compounds were named following IUPAC rules as applied by Beilstein-Institut AutoNom (version 2.1), a software for systematic names in organic chemistry.

C-(4-Phenyl-chroman-2-yl)methylamine (12). A solution of **11**¹⁷ (2.0 g, 4.79 mmol) in 4.4% HCOOH–MeOH (75 mL) was added dropwise to a mixture of 10% Pd/C (4.0 g) in 4.4% HCOOH–MeOH (150 mL). The mixture was stirred overnight under a nitrogen atmosphere. After the catalyst was filtered off and washed with MeOH, the solvent was evaporated and the residue was taken up with 2 N NaOH and extracted with CHCl₃. The dried solvents were evaporated to give an oil; 0.6 g (52% yield). ¹H NMR (CDCl₃): δ 1.72 (br s, 2, NH₂, exchangeable with D₂O), 1.8–2.29 (m, 2, 3-H), 2.7–3.02 (m, 2, CH₂N), 4.03–4.41 (m, 2, 2-H and 4-H), 6.59–7.32 (m, 9, ArH).

cis-2-(2,6-Dimethoxy-phenoxy)-N-(4-phenyl-chroman-2-ylmethyl)acetamide (13). Ethyl chloroformate (0.13 g, 1.13 mmol) was added dropwise to a stirred and cooled (0 °C) solution of (2,6-dimethoxy-phenoxy)acetic acid¹⁸ (0.24 g, 1.13 mmol) and Et₃N (0.12 g, 1.13 mmol) in CHCl₃ (10 mL), followed after 30 min by the addition of a solution of **12** (0.27 g, 1.13 mmol) in CHCl₃ (6 mL). The resulting reaction mixture was stirred at room temperature overnight and then washed with 2 N HCl, 2 N NaOH, and finally water. Removal of dried solvents gave an oil, which was purified by column chromatography. Eluting with cyclohexanes–Et₂O (5:5) gave **13** as a solid; 0.35 g (71% yield); mp 44–52 °C. ¹H NMR (CDCl₃): δ 1.95 (dt, $J = 11.9, 13.4$ Hz, 1, 3-H), 2.21 (ddd, $J = 1.5, 5.8, 13.4$ Hz, 1, 3-H), 3.49–3.92 (m, 2, CH₂N), 3.86 (s, 6, OCH₃), 4.19 (dd, $J = 11.9, 5.8$ Hz, 1, 4-H), 4.34 (m, 1, 2-H), 4.61 (s, 2, CH₂O), 6.54–7.38 (m, 12, ArH), 8.32 (br t, 1, NH, exchangeable with D₂O).

cis-[2-(2,6-Dimethoxy-phenoxy)ethyl]-(4-phenyl-chroman-2-ylmethyl)amine Oxalate (5). A solution of 10 M BH₃·CH₃SCH₃ (0.09 mL) in dry diglyme (1.5 mL) was added dropwise at room temperature to a solution of **13** (0.31 g, 0.72 mmol) in dry diglyme (16 mL) with stirring under a stream of dry nitrogen with exclusion of moisture. When the addition was completed, the reaction mixture was heated at 120 °C for 6 h. After the mixture was cooled at 0 °C, excess borane was destroyed by cautious dropwise addition of MeOH (7 mL). The resulting mixture was left to stand overnight at room temperature, cooled at 0 °C, treated with HCl gas for 10 min, and then heated at 120 °C for 4 h. Removal of the solvent under reduced pressure gave a residue, which was dissolved in water. The aqueous solution was basified with NaOH pellets and extracted with CHCl₃. Removal of dried solvents gave a residue, which was purified by column chromatography. Eluting with cyclohexanes–EtOAc–EtOH (8:1.5:0.5) afforded **5** as the free base; 0.25 g (83% yield). ¹H NMR (CDCl₃): δ 2.01 (dt, $J = 13.1, 11.8$ Hz, 1, 3-H), 2.28 (ddd, $J = 1.3, 5.7, 13.1$ Hz, 1, 3-H), 3.03 (m, 4, CH₂NCH₂), 3.52 (br s, 1, NH, exchangeable with D₂O), 3.85 (s, 6, OCH₃), 4.21 (m, 3, 4-H and CH₂O), 4.49 (m, 1, 2-H), 6.54–7.39 (m, 12, ArH). The free base was transformed into the oxalate salt and crystallized from EtOH; mp 160–161 °C. Anal. (C₂₆H₂₉NO₄·H₂C₂O₄) C, H, N.

cis- and trans-4-Phenyl-thiochroman-2-carboxylic Acid (14). A mixture of *cis*- and *trans*-4-phenyl-thiochroman-2-carboxylic acid ethyl ester¹⁹ (0.7 g, 2.35 mmol) and 2 N NaOH (9.5 mL) was heated to 80 °C for 6 h. The mixture was

extracted with CHCl₃, and the aqueous layer was acidified with concentrated HCl. Extraction with CHCl₃, followed by washing, drying, and evaporation of the extracts, gave **14** as a *cis/trans* mixture (ratio 1:1); 0.58 g (92% yield); mp 145–162 °C. ¹H NMR (CDCl₃): δ 2.3–2.78 (m, 4, 3-H; *cis* and *trans*), 3.9 (dd, 1, 4-H; *trans*), 4.03 (dd, 1, 4-H; *cis*), 4.27 (dd, 1, 2-H; *trans*), 4.38 (br t, 1, 2-H; *cis*), 6.36 (br s, 2, COOH, exchangeable with D₂O; *cis* and *trans*), 6.62–7.41 (m, 18, ArH; *cis* and *trans*).

cis- and trans-4-Phenyl-thiochroman-2-carboxylic Acid [2-(2,6-Dimethoxy-phenoxy)ethyl]amide (16 and 17). Ethyl chloroformate (0.83 g, 7.40 mmol) was added dropwise to a stirred and cooled (0 °C) solution of **14** (2.0 g, 7.40 mmol) and Et₃N (0.76 g, 7.40 mmol) in CHCl₃ (85 mL), followed after 30 min by the addition of a solution of 2-(2,6-dimethoxy-phenoxy)ethylamine²¹ (1.46 g, 7.40 mmol) in CHCl₃ (50 mL). The resulting reaction mixture was stirred at room temperature for 3 h and then washed with 2 N HCl, 2 N NaOH, and finally water. Removal of dried solvents gave an oil, which was purified by column chromatography using petroleum ether–Et₂O (4:6) as the eluent. The *trans* isomer **16** eluted first; 1.5 g (45% yield). ¹H NMR (CDCl₃): δ 2.54 (m, 2, 3-H), 3.52 (m, 2, NCH₂), 3.76 (s, 6, OCH₃), 3.81 (m, 1, 4-H), 4.09 (m, 2, CH₂O), 4.26 (t, 1, 2-H), 6.52–7.33 (m, 12, ArH), 7.56 (br t, 1, NH, exchangeable with D₂O).

The second fraction was the *cis* isomer **17** as an oil; 0.86 g (26% yield). ¹H NMR (CDCl₃): δ 2.41 (dt, $J = 11.0, 13.4$ Hz, 1, 3-H), 2.68 (dt, $J = 4.0, 13.4$ Hz, 1, 3-H), 3.50 (m, 2, NCH₂), 3.85 (s, 6, OCH₃), 4.09 (m, 3, CH₂O and 4-H), 4.21 (dd, $J = 4.0, 11.0$ Hz, 1, 2-H), 6.55–7.40 (m, 12, ArH), 7.51 (br t, 1, NH, exchangeable with D₂O).

trans-[2-(2,6-Dimethoxy-phenoxy)ethyl]-(4-phenyl-thiochroman-2-ylmethyl)amine Oxalate (6). This was synthesized from **16** (1.0 g, 2.22 mmol) following the procedure described for **5**. Eluting with cyclohexanes–EtOAc–EtOH (8:1.5:0.5) afforded **6** as the free base; 0.6 g (62% yield). ¹H NMR (CDCl₃): δ 1.93 (br s, 1, NH, exchangeable with D₂O), 2.13 (ddd, $J = 4.4, 11.1, 13.5$ Hz, 1, 3-H), 2.40 (ddd, $J = 3.3, 4.8, 13.5$ Hz, 1, 3-H), 2.78–2.98 (m, 4, CH₂NCH₂), 3.29 (m, 1, 2-H), 3.75 (s, 6, OCH₃), 4.10 (t, 2, CH₂O), 4.33 (t, 1, 4-H), 6.52–7.33 (m, 12, ArH). The free base was transformed into the oxalate salt and crystallized from EtOH–MeOH; mp 198–199 °C. Anal. (C₂₆H₂₉NO₃·0.5H₂C₂O₄·0.25H₂O) C, H, N, S.

cis-[2-(2,6-Dimethoxy-phenoxy)ethyl]-(4-phenyl-thiochroman-2-ylmethyl)amine Oxalate (7). This was synthesized from **17** (0.57 g, 1.27 mmol) following the procedure described for **5**. Eluting with cyclohexanes–EtOAc–EtOH (8:1.5:0.5) afforded **7** as the free base; 0.43 g (78% yield). ¹H NMR (CDCl₃): δ 1.92 (br s, 1, NH, exchangeable with D₂O), 2.02 (ddd, $J = 10.5, 12.3, 13.3$ Hz, 1, 3-H), 2.51 (dt, $J = 3.8, 13.3$ Hz, 1, 3-H), 2.77–3.03 (m, 4, CH₂NCH₂), 3.70 (m, 1, 2-H), 3.82 (s, 6, OCH₃), 4.07 (m, 1, 4-H), 4.13 (t, 2, CH₂O), 6.53–7.41 (m, 12, ArH). The free base was transformed into the oxalate salt and crystallized from EtOH–Et₂O; mp 114–115 °C. Anal. (C₂₆H₂₉NO₃·H₂C₂O₄·0.75H₂O) C, H, N, S.

cis-4-Phenyl-1,2,3,4-tetrahydro-naphthalene-2-carboxylic Acid [2-(2,6-Dimethoxy-phenoxy)ethyl]amide (18). Ethyl chloroformate (0.24 g, 2.14 mmol) was added dropwise to a stirred and cooled (0 °C) solution of *cis*-4-phenyl-1,2,3,4-tetrahydro-naphthalen-2-carboxylic acid²⁰ (0.54 g, 2.14 mmol) and Et₃N (0.22 g, 2.14 mmol) in CHCl₃ (25 mL), followed after 30 min by the addition of a solution of 2-(2,6-dimethoxy-phenoxy)ethylamine²¹ (0.42 g, 2.14 mmol) in CHCl₃ (15 mL). The resulting reaction mixture was stirred at room temperature for 3 h and then washed with 2 N HCl, 2 N NaOH, and finally water. Removal of dried solvent gave an oil, which was purified by column chromatography. Eluting with petroleum ether–cyclohexanes–EtOAc (2.5:2.5:5) gave **18** as a solid; 0.85 g (92% yield); mp 115–117 °C. ¹H NMR (CDCl₃): δ 2.03 (dt, $J = 11.1, 12.5$ Hz, 1, 3-H), 2.36 (ddd, $J = 3.5, 4.4, 13.8$ Hz, 1, 3-H), 2.72 (m, 1, 2-H), 2.92–3.32 (m, 2, 1-H), 3.57 (q, 2, NCH₂), 3.80 (s, 6, OCH₃), 4.12 (m, 3, CH₂O and 4-H), 6.53–7.36 (m, 12, ArH), 6.94 (br t, 1, NH, exchangeable with D₂O).

cis-[2-(2,6-Dimethoxy-phenoxy)ethyl]-(4-phenyl-1,2,3,4-tetrahydro-naphthalen-2-ylmethyl)amine Oxalate (9).

This was synthesized from **18** (0.85 g, 1.97 mmol) following the procedure described for **5**. Eluting with cyclohexanes–EtOAc–EtOH (8:1.5:0.5) afforded **9** as the free base; 0.58 g (71% yield). ¹H NMR (CDCl₃): δ 1.56 (dt, *J* = 12.45, 12.1 Hz, 1, 3-H), 1.86 (br s, 1, NH, exchangeable with D₂O), 2.04–2.36 (m, 2, 2-H and 3-H), 2.58–3.10 (m, 6, 1-H and CH₂NCH₂), 3.80 (s, 6, OCH₃), 4.10 (m, 1, 4-H), 4.17 (t, 2, CH₂O), 6.52–7.36 (m, 12, ArH). The free base was transformed into the oxalate salt and crystallized from MeOH; mp 200 °C. Anal. (C₂₇H₃₁NO₃·0.5H₂C₂O₄·0.25H₂O) C, H, N.

cis-2-[[2-(2,6-Dimethoxy-phenoxy)ethylamino]methyl]-4-phenyl-3,4-dihydro-2H-naphthalen-1-one Hydrochloride (8). A solution of 4-phenyl-1-tetralone²² (0.95 g, 4.28 mmol), 2-(2,6-dimethoxy-phenoxy)ethylamine·HCl²¹ (1.0 g, 4.28 mmol), paraformaldehyde (0.39 g, 13.0 mmol), and concentrated HCl (0.1 mL) was heated at reflux for 8 h. After evaporation of the solvent, the residue was dissolved in 2 N NaOH and extracted with CHCl₃. Removal of dried solvents gave an oil, which was purified by column chromatography. Eluting with cyclohexane–acetone (5:5) gave a mixture of *cis* and *trans* isomers; 1.31 g (71% yield). The mixture of free bases was transformed into the hydrochloride salt. Following crystallization from 2-PrOH/Et₂O, only the *cis* isomer was isolated; 0.3 g; mp 161–163 °C. ¹H NMR (CDCl₃ + D₂O): δ 2.10 (dd, *J* = 13.5, 12.5 Hz, 1, 3-H), 2.40 (dt, *J* = 13.5, 4.2 Hz, 1, 3-H), 3.08–3.50 (m, 4, CH₂NCH₂), 3.87 (s, 6, OCH₃), 3.96 (m, 1, 2-H), 4.2–4.5 (m, 3, 4-H and CH₂O), 6.55–8.1 (m, 12, ArH). Anal. (C₂₇H₂₉NO₄·HCl·0.25H₂O) C, H, N.

(2-Benzyl-phenoxy)acetaldehyde Dimethyl Acetal (19). A 60% NaH dispersion in mineral oil (0.24 g, 6.0 mmol) was washed with hexane under nitrogen, suspended in dimethylformamide (DMF; 0.54 mL), and then added over 15 min of a solution of 2-benzyl-phenol (1.0 g, 5.43 mmol) in dry DMF (0.76 mL). The mixture was stirred at room temperature for 1.5 h and cooled to 0 °C. Chloroacetaldehyde dimethyl acetal (0.77 g, 6.18 mmol) was added, and the reaction mixture was heated at 120 °C for 8 h. After it was cooled, the mixture was poured in 2 N NaOH (10 mL) and extracted with Et₂O. Removal of dried solvents gave a residue, which was purified by column chromatography. Eluting with cyclohexanes–EtOAc (98:2) gave an oil; 0.53 g (36% yield). ¹H NMR (CDCl₃): δ 3.42 (s, 6, OCH₃), 3.99 (d, 2, OCH₂), 4.01 (s, 2, CH₂Ar), 4.68 (t, 1, CH), 6.81–7.30 (m, 9, ArH).

(2-Benzyl-phenoxy)acetaldehyde (20). Compound **19** (0.53 g, 1.95 mmol) was added to a solution of 2 N HCl (3.2 mL) in acetone (5.4 mL), and the resulting solution was heated to 70 °C for 1.5 h with stirring. After it was cooled, Et₂O (22 mL) and H₂O (9.0 mL) were added. The ether layer was separated and washed with 5% Na₂CO₃ (1 × 25 mL) and H₂O (2 × 25 mL). Removal of dried solvents gave a residue, which was purified by column chromatography. Eluting with cyclohexanes–EtOAc (8:2) gave a solid; 0.3 g (68% yield); mp 42–43 °C. ¹H NMR (CDCl₃): δ 4.06 (s, 2, CH₂Ar), 4.51 (d, 2, OCH₂), 6.68–7.32 (m, 9, ArH), 9.76 (d, 1, CHO).

[2-(2-Benzyl-phenoxy)ethyl]-[2-(2,6-dimethoxy-phenoxy)ethyl]amine Oxalate (10). A 2.03 M solution of HCl gas in EtOH (1.31 mL) was added to a solution of 2-(2,6-dimethoxy-phenoxy)ethylamine²¹ (1.56 g, 7.91 mmol) and **20** (0.3 g, 1.33 mmol) in EtOH (10 mL), followed by the addition of NaBH₃CN (0.077 g, 1.16 mmol) and molecular sieves (4 Å). The mixture was stirred at room temperature for 4 h, then acidified at pH 1 with 2 N HCl, filtered, and evaporated. The residue was taken up with water and basified with 6 N KOH, and the mixture was extracted with Et₂O. After it was dried, the solvent was evaporated and the residue was purified by column chromatography. Eluting with EtOAc–EtOH (9:1) gave **10** as the free base; 0.3 g (56% yield). ¹H NMR (CDCl₃): δ 3.03 and 3.1 (two t, 4, CH₂NCH₂), 3.8 (s, 6, OCH₃), 3.98 (s, 2, CH₂Ar), 4.17 (m, 4, OCH₂ and CH₂O), 6.55–7.28 (m, 12, ArH). The free base was transformed into the oxalate salt and crystallized from EtOH; mp 170–171 °C. Anal. (C₂₅H₂₉NO₄·H₂C₂O₄) C, H, N.

Molecular Modeling. Molecular models of ligands **3–5** were built starting from the X-ray crystallographic coordinates

of **1**, retrieved from the Cambridge Crystallographic Database (refcode BAXBEH),⁴⁶ by using the fragment library implemented in the QXP software.⁴⁷ For compounds **3** and **5**, the (*S*)-equatorial configuration was adopted according to the X-ray data of **1**.⁴⁸

For the 3D receptor model, the coordinates of the rat α_{1A}-AR subtype in its activated state were recovered from our recent paper.⁴² Because site-directed mutagenesis studies⁴⁹ strongly suggested that Asp170 binds to the charged nitrogen of both agonist and antagonist ligands, **1** was initially placed into the cavity of the receptor delimited by transmembrane domains 3–7 with the charged amino group at a proper distance from the carboxylate anion of Asp170 to make a hydrogen bond with it and with the dimethoxyphenoxy group pointing toward the extracellular loops. This initial complex was then minimized with the Pollak–Ribiere conjugate gradient method until the root mean square gradient was lower than 0.001 kcal/mol Å². A distance-dependent dielectric constant of 4 r was used throughout the calculations. At this step, the Cα trace of the receptor backbone was kept fixed. Compounds **3–5** were then overlaid onto the structure of **1**, extracted from the previous minimization step, with the module TFIT of QXP. TFIT allows a flexible superposition of one or more molecules on a selected template using a superposition force field, which automatically assigns short-range attractive forces to similar atoms in different molecules. A first flexible docking run was performed on **4** using the MCDOCK module of QXP. All of the residues in a region within 5.0 Å from all of the ligand atoms were allowed to move whereas the rest of the protein was kept fixed. A total of 1000 different random positions of the ligand in the receptor were generated and subjected to a Monte Carlo simulation, followed again by a Pollak–Ribiere conjugate gradient minimization. During the energy minimization, constrained atom pairs were defined as the ligand-protonated nitrogen atom and the Oδ1 atom of Asp170. A quadratic energy potential of 1.2 kcal/mol Å² was applied to them. The receptor structure obtained at the end of this run was then used as the starting model for a new series of ligand docking runs. During the simulation, the receptor was kept fixed, the ligands were allowed to freely move, and no constrained atom pairs were used. The binding energy was calculated as the sum of the receptor–ligand nonbonded energy, the relative internal ligand energy, and the energy, relative to the local minima, of the binding site. QXP uses a mixed AMBER/MM2 force field to estimate the binding energy of the receptor–ligand complex. The lowest energy receptor–ligand complexes were retrieved and reported in Figure 2. For binding energy calculation within GRID, the directive FOBE and TORS were set to 4.0 and 1.0 kcal/mol, respectively. The modeling and docking calculations were carried out on an SGI-O2 workstation R10000. The graphical representations of the protein models in Figure 2 are drawn with the MOLSCRIPT software package.⁵⁰

Biology. Functional Antagonism in Isolated Tissues.

Male Wistar rats (275–300 g) were killed by cervical dislocation, and the organs required were isolated, freed from adhering connective tissue, and set up rapidly under a suitable resting tension in 20 mL organ baths containing physiological salt solution kept at 37 °C and aerated with 5% CO₂:95% O₂ at pH 7.4. Concentration–response curves were constructed by cumulative addition of agonist. The concentration of agonist in the organ bath was increased approximately 3-fold at each step, with each addition being made only after the response to the previous addition had attained a maximal level and remained steady. Contractions were recorded by means of a force displacement transducer connected to the MacLab system PowerLab/800. In addition, parallel experiments in which tissues did not receive any antagonist were run in order to check any variation in sensitivity.

Rat Prostate. This tissue was used to assess α_{1A}-adrenergic antagonism.²⁶ Prostate strips measuring 8–10 mm in length and 1–2 mm in width were mounted under 2 g of tension in modified Krebs' solution of the following composition (mM): NaCl, 118; KCl, 4.7; KH₂PO₄, 1.18; NaHCO₃, 25; CaCl₂, 2.5;

MgSO₄·7H₂O, 1.18; glucose, 5.55. The preparations were equilibrated for 60 min with washing every 20 min. Before the concentration–response curves were started, tissues were exposed to (–)-noradrenaline at a concentration of 1.0 μM. A minimum response of 0.5 g of tension was required for the tissue to be used for concentration–response curves. After a 90 min wash period, a cumulative concentration–response curve to (–)-noradrenaline was constructed. After it was washed for 90 min, the antagonist was allowed to equilibrate with the tissue for 30 min, and then, a new concentration–response curve to the agonist was obtained. (–)-Noradrenaline solutions contained 0.05% Na₂S₂O₅ to prevent oxidation.

Rat Vas Deferens Prostatic Portion. This tissue was used to assess α_{1A}-adrenergic antagonism.²⁷ Prostatic portions of 2 cm length were mounted under 0.5 g of tension in Tyrode solution of the following composition (mM): NaCl, 130.0; KCl, 2.0; CaCl₂, 1.8; MgCl₂, 0.89; NaHCO₃, 25.0; NaH₂PO₄, 0.42; glucose, 5.6. Cocaine hydrochloride (0.1 μM) was added to the Tyrode to prevent the neuronal uptake of (–)-noradrenaline. The preparations were equilibrated for 60 min with washing every 15 min. After the equilibration period, tissues were primed two times by addition of 10 μM (–)-noradrenaline. After another washing and equilibration period of 60 min, a (–)-noradrenaline concentration–response curve was constructed (basal response). The antagonist was allowed to equilibrate with the tissue for 30 min, followed by 30 min of washing. Then, a new concentration–response curve to the agonist was obtained. (–)-Noradrenaline solutions contained 0.05% Na₂S₂O₅ to prevent oxidation.

Rat Spleen. This tissue was used to assess α_{1B}-adrenergic antagonism.^{28b} The spleen was removed and bisected longitudinally into two strips, which were suspended in tissue baths containing Krebs solution of the following composition (mM): NaCl, 120.0; KCl, 4.7; CaCl₂, 2.5; MgSO₄, 1.5; NaHCO₃, 20.0; KH₂PO₄, 1.2; glucose, 11.0; K₂ethylenediaminetetraacetic acid (EDTA), 0.01. (±)-Propranolol hydrochloride (4.0 μM) was added to block β-ARs. The spleen strips were placed under 1 g of resting tension and equilibrated for 2 h. The cumulative concentration–response curves to (–)-phenylephrine were measured isometrically and obtained at 30 min intervals; the first one was discarded, and the second one was taken as the control. The antagonist was allowed to equilibrate with the tissue for 30 min, followed by 30 min of washing. Then, a new concentration–response curve to the agonist was constructed.

Rat Aorta. This tissue was used to assess α_{1D}-adrenergic antagonism.^{28a} Thoracic aorta was cleaned from extraneous connective tissue and placed in Krebs solution of the following composition (mM): NaCl, 118.4; KCl, 4.7; CaCl₂, 1.9; MgSO₄, 1.2; NaHCO₃, 25.0; NaH₂PO₄, 1.2; glucose, 11.7. Cocaine hydrochloride (0.1 μM) and (±)-propranolol hydrochloride (4.0 μM) were added to prevent the neuronal uptake of (–)-noradrenaline and to block β-ARs, respectively. Two helicoidal strips (15 mm × 3 mm) were cut from each aorta beginning from the end most proximal to the heart. The endothelium was removed by rubbing with filter paper; the absence of acetylcholine (100 μM)-induced relaxation to preparations contracted with (–)-noradrenaline (1 μM) was taken as an indicator that the vessel was denuded successfully. Vascular strips were then tied with surgical thread and suspended in a jacketed tissue bath containing Tyrode solution. Strips were secured at one end to Plexiglas hooks and connected to a transducer for monitoring changes in isometric contraction. After at least 2 h equilibration period under an optimal tension of 2 g, cumulative (–)-noradrenaline concentration–response curves were recorded at 1 h intervals; the first two were discarded, and the third one was taken as the control. The antagonist was allowed to equilibrate with the tissue for 30 min before the generation of the fourth cumulative concentration–response curve to (–)-noradrenaline. (–)-Noradrenaline solutions contained 0.05% K₂EDTA and 0.9% NaCl to prevent oxidation.

Radioligand Binding Assays. Binding to cloned human α₁-AR subtypes was performed in membranes from CHO cells transfected by electroporation with DNA expressing the gene

encoding each α₁-AR subtype. Cloning and stable expression of the human α₁-AR gene was performed as previously described.²³ CHO cell membranes (30 μg proteins) were incubated in 50 mM Tris-HCl, pH 7.4, with 0.1–0.4 nM [³H]prazosin, in a final volume of 1.02 mL for 30 min at 25 °C, in absence or presence of competing drugs (1 pM–10 μM). Nonspecific binding was determined in the presence of 10 μM phentolamine. The incubation was stopped by addition of ice-cold Tris-HCl buffer and rapid filtration through 0.2% polyethyleneimine pretreated Whatman GF/B or Schleicher & Schuell GF52 filters. Genomic clone G-21 coding for the human 5-HT_{1A} receptor was stably transfected in a human cell line (HeLa).²⁴ HeLa cells were grown as monolayers in Dulbecco's modified Eagle's medium (DMEM), supplemented with 10% fetal calf serum and gentamicin (100 μg/mL), and 5% CO₂ at 37 °C. Cells were detached from the growth flask at 95% confluence by a cell scraper and were lysed in ice-cold Tris 5 mM and EDTA 5 mM buffer (pH 7.4). Homogenates were centrifuged at 40 000g for 20 min, and pellets were resuspended in a small volume of ice-cold Tris 5 mM and EDTA 5 mM buffer (pH 7.4) and immediately frozen and stored at –70 °C until use. On the experimental day, cell membranes were resuspended in binding buffer: 50 mM Tris-HCl (pH 7.4), 2.5 mM MgCl₂, and 10 μM pargiline.²⁵ Membranes were incubated in a final volume of 1 mL for 30 min at 30 °C with 0.7–1.4 nM [³H]8-OH-DPAT, in the absence or presence of competing drugs. Nonspecific binding was determined in the presence of 10 μM 5-HT. The incubation was stopped by the addition of ice-cold Tris-HCl buffer and rapid filtration through 0.2% polyethyleneimine-pretreated Whatman GF/B or Schleicher & Schuell GF52 filters.

Data Analysis. In functional studies, responses were expressed as percentage of the maximal contraction observed in the agonist concentration–response curve taken as a control. Pharmacological computer programs analyzed the agonist concentration–response curves. pA₂ values were calculated according to Arunlakshana and Schild^{51a} from the dose ratios at the EC₅₀ values of the agonists calculated at three antagonist concentrations. Each concentration was tested five times, and Schild plots were constrained to slope –1, as required by theory.^{51b} When this method was applied, it was always verified that the experimental data generated a line whose derived slope was not significantly different from unity (*p* > 0.05). In a number of cases, Schild analysis could not be performed due to depression of the maximal response by high antagonist concentrations and the resulting nonparallel slopes of the concentration–response curves. Consequently, pK_B values were calculated from only one concentration. Compounds 2–10 were tested in isolated rat prostate at only one concentration, in the range of 0.01–1 μM, when determining α_{1A}-AR blocking activity. In these cases, pK_B values were calculated according to van Rossum.^{51c}

Binding data were analyzed using the nonlinear curve-fitting program Allfit.⁵² Scatchard plots were linear in all preparations. All pseudo-Hill coefficients (nH) were not significantly different from unity (*p* > 0.05). Equilibrium inhibition constants (*K_i*) were derived from the Cheng–Prusoff equation,⁵³ $K_i = IC_{50}/(1 + L/K_d)$, where *L* and *K_d* are the concentration and the equilibrium dissociation constant of the radioligand. p*K_i* values are the mean ± SE of 2–3 separate experiments performed in triplicate.

Acknowledgment. This paper was supported by grants from the Universities of Camerino, Bari, and Bologna and MURST.

References

- (1) For part 6, see ref 12.
- (2) (a) Bylund, D. B.; Eikenberg, D. C.; Hieble, J. P.; Langer, S. Z.; Lefkowitz, R. J.; Minneman, K. P.; Molinoff, P. B.; Ruffolo, R. R., Jr.; Trendelenburg, U. IV. International Union of Pharmacology Nomenclature of Adrenoceptors. *Pharmacol. Rev.* **1994**, *46*, 121–136. (b) Hieble, J. P.; Bylund, D. B.; Clarke, D. E.;

- Eikenburg, D. C.; Langer, S. Z.; Lefkowitz, R. J.; Minneman, K. P.; Ruffolo, R. R. International Union of Pharmacology X. Recommendation for Nomenclature of α_1 -Adrenoceptors: Consensus Update. *Pharmacol. Rev.* **1995**, *47*, 267–270.
- (3) Faure, C.; Pimoule, C.; Arbillia, S.; Langer, S. Z.; Graham, D. Expression of α_1 -Adrenoceptor Subtypes in Rat Tissues: Implications for α_1 -Adrenoceptor Classification. *Eur. J. Pharmacol. Mol. Pharmacol.* **1994**, *268*, 141–149.
- (4) Ford, A. P. D. W.; Williams, T. J.; Blue, D. R.; Clarke, D. E. α_1 -Adrenoceptor Classification: Sharpening Occam's Razor. *Trends Pharmacol. Sci.* **1994**, *15*, 167–170.
- (5) (a) Kenny, B.; Ballard, S.; Blagg, J.; Fox, D. Pharmacological Options in the Treatment of Benign Prostatic Hyperplasia. *J. Med. Chem.* **1997**, *40*, 1293–1315. (b) Leonardi, A.; Testa, R.; Motta, G.; De Benedetti, P. G.; Hieble, P.; Giardinà, D. α_1 -Adrenoceptors: Subtype- and Organ-Selectivity of Different Agents. In *Perspective in Receptor Research*; Giardinà, D., Piergentili, A., Pignini, M., Eds.; Elsevier: Amsterdam, 1996; pp 135–152. (c) Ruffolo, R. R., Jr.; Bondinell, W.; Hieble, J. P. α - and β -Adrenoceptors. From the Gene to the Clinic. 2. Structure–Activity Relationships and Therapeutic Applications. *J. Med. Chem.* **1995**, *38*, 3681–3716.
- (6) Matyus, P.; Horvath, K. α -Adrenergic Approach in the Medical Management of Benign Prostatic Hyperplasia. *Med. Res. Rev.* **1997**, *17*, 523–535.
- (7) (a) Nasu, K.; Moriyama, N.; Kawabe, K.; Tsujimoto, G.; Murai, M.; Tanaka, T.; Yano, J. Quantification and Distribution of α_1 -Adrenoceptor Subtype mRNAs in Human Prostate: Comparison of Benign Hypertrophied Tissue and Non-Hypertrophied Tissue. *Br. J. Pharmacol.* **1996**, *119*, 797–803. (b) Price, D. T.; Scwhinn, D. A.; Lomasney, J. W.; Allen, L. F.; Caron, M. G.; Lefkowitz, R. J. Identification, Quantitation, and Localization of mRNA for Three Distinct Alpha-1 Adrenergic Subtypes in Human Prostate. *J. Urol.* **1993**, *150*, 546–551.
- (8) Cavalli, A.; Lattion, A.-L.; Hummler, E.; Nenniger, M.; Pedrazzini, T.; Aubert, J.-F.; Michel, M. C.; Yang, M.; Lembo, G.; Vecchine, C.; Mostardini, M.; Schmidt, A.; Beermann, F.; Cotecchia, S. Decreased Blood Pressure Response in Mice Deficient of the α_{1B} -Adrenergic Receptor. *Proc. Natl. Acad. Sci. U.S.A.* **1997**, *94*, 11589–11594.
- (9) Malloy, B. J.; Price, D. T.; Price, R. R.; Bienstock, A. M.; Dole, M. K.; Funk, B. L.; Rudner, X. L.; Richardson, C. D.; Donatucci, C. F.; Schwinn, D. A. α_1 -Adrenergic Receptor Subtypes in Human Detrusor. *J. Urol.* **1998**, *160*, 937–943.
- (10) Broten, T.; Scott, A.; Siegl, P. K. S.; Furray, C.; Lagu, B.; Nagarathnam, W. C.; Marzabadi, W. M.; Murali Dhar, T. G.; Gluckowski, C. Alpha-1 Adrenoceptor Blockade Inhibits Detrusor Instability in Rats With Bladder Outlet Obstruction. *FASEB J. Abstr.* **1998**, *12*, A445.
- (11) Meyer, M. D.; Altenbach, R. J.; Basha, F. Z.; Carrol, W. A.; Condon, S.; Elmore, S. W.; Kerwin, J. F., Jr.; Sippy, K. B.; Tietje, K.; Wendt, M. D.; Hancock, A. A.; Brune, M. E.; Buckner, S. A.; Drizin, I. Structure–Activity Studies for a Novel Series of Tricyclic Substituted Hexahydrobenzo[e]isoindole α_{1A} Adrenoceptor Antagonists as Potential Agent for the Symptomatic Treatment of Benign Prostatic Hyperplasia (BPH). *J. Med. Chem.* **2000**, *43*, 1586–1603.
- (12) Quaglia, W.; Pignini, M.; Piergentili, A.; Giannella, M.; Marucci, G.; Poggesi, E.; Leonardi, A.; Melchiorre, C. Structure–Activity Relationships in 1,4-Benzodioxan-Related Compounds. 6. Role of the Dioxane Unit on Selectivity for α_1 -Adrenoceptor Subtypes. *J. Med. Chem.* **1999**, *42*, 2961–2968 and references therein.
- (13) For example, see Melchiorre, C.; Belleau, B. *Adrenoceptors and Catecholamine Action*, Part A; Kunos, G., Ed.; Wiley: New York, 1981; pp 131–179.
- (14) Melchiorre, C.; Brasili, L.; Giardinà, D.; Pignini, M.; Strappaghetta, G. 2-[[[2-(2,6-Dimethoxyphenoxy)ethyl]amino]methyl]-1,4-benzoxathian: a New Antagonist with High Potency and Selectivity Toward α_1 -Adrenoceptors. *J. Med. Chem.* **1984**, *27*, 1535–1536.
- (15) Pignini, M.; Brasili, L.; Giannella, M.; Giardinà, D.; Gulinì, U.; Quaglia, W.; Melchiorre, C. Structure–Activity Relationships in 1,4-Benzodioxan-Related Compounds. Investigation on the Role of the Dehydrodioxane Ring on α_1 -Adrenoceptor Blocking Activity. *J. Med. Chem.* **1988**, *31*, 2300–2304.
- (16) (a) Quaglia, W.; Pignini, M.; Giannella, M.; Melchiorre, C. 3-Phenyl Analogues of 2-[[[2-(2,6-Dimethoxyphenoxy)ethyl]amino]methyl]-1,4-benzodioxan (WB 4101) as Highly Selective α_1 -Adrenoceptor Antagonists. *J. Med. Chem.* **1990**, *33*, 2946–2948. (b) Quaglia, W.; Pignini, M.; Tayebati, S. K.; Piergentili, A.; Giannella, M.; Marucci, G.; Melchiorre, C. Structure–Activity Relationships in 1,4-Benzodioxan-Related Compounds. 4. Effect of Aryl and Alkyl Substituents at Position 3 on α -Adrenoceptor Blocking Activity. *J. Med. Chem.* **1993**, *36*, 1520–1528. (c) Quaglia, W.; Pignini, M.; Tayebati, S. K.; Piergentili, A.; Giannella, M.; Leonardi, A.; Taddei, C.; Melchiorre, C. Synthesis, Absolute Configuration, and Biological Profile of the Enantiomers of *trans*-[2-(2,6-Dimethoxyphenoxy)ethyl][3-*p*-tolyl-2,3-dihydro-1,4-benzodioxin-2-yl)methyl]amine (Mephendioxan), a Potent Competitive α_{1A} -Adrenoceptor Antagonist. *J. Med. Chem.* **1996**, *39*, 2253–2258.
- (17) Sime, J. T.; Ainsworth, A. T. Chroman Derivatives and Pharmaceutical Compositions Containing Them. Eur. Pat. Appl. 20,018, 1980; *Chem. Abstr.* **1981**, *94*, 174883w.
- (18) Berhenke, L. F.; Bein, L. E. Aryloxy Aliphatic Carboxylates. U.S. Patent 2,516,611, 1950; *Chem. Abstr.* **1951**, *45*, 661b.
- (19) Ishibashi, H.; Okada, M.; Sato, K.; Ikeda, M.; Ishiyama, K.; Tamura, Y. Cationic Polar Cycloadditions of Phenylthionium Ions with Olefins: A New Route to Thiochromans. *Chem. Pharm. Bull.* **1985**, *33*, 90–95.
- (20) Holava, H. M.; Partyka, R. A. 1-Phenyl-3-(aminoalkyl)-1,2,3,4-tetrahydronaphthalenes and Their Salts as Neuroleptic Agents or Central Nervous System Stimulants. U.S. Patent 3,663,608, 1972; *Chem. Abstr.* **1972**, *77*, 61675k and references therein.
- (21) Woolley, D. W. Probable Evolutionary Relations of Serotonin and Indole-Acetic Acid, and Some Practical Consequences Therefrom. *Nature* **1957**, *10*, 630–633.
- (22) Miyano, S.; Tatsuoka, T.; Suzuki, K.; Imao, K.; Satoh, F.; Ishihara, T.; Hirotsu, I.; Kihara, T.; Hatta, M.; Horikawa, Y.; Sumoto, K. The Synthesis and Antilipidperoxidation Activity of 4,4-Diarylbutylamines and 4,4-Diarylbutanamides. *Chem. Pharm. Bull.* **1990**, *38*, 1570–1574.
- (23) Testa, R.; Taddei, C.; Poggesi, E.; Destefani, C.; Cotecchia, S.; Hieble, J. P.; Sulpizio, A. C.; Naselsky, D.; Bergsma, D.; Ellis, S.; Swift, A.; Ganguly, S.; Ruffolo, R. R.; Leonardi, A. Rec 15/2739 (SB 216469): a Novel Prostate Selective α_1 -Adrenoceptor Antagonist. *Pharmacol. Commun.* **1995**, *6*, 79–86.
- (24) Fargin, A.; Raymond, J. R.; Regan, J. W.; Cotecchia, S.; Lefkowitz, R. J.; Caron, M. G. Effector Coupling Mechanisms of the Cloned 5-HT_{1A} Receptor. *J. Biol. Chem.* **1989**, *264*, 14848–14852.
- (25) Fargin, A.; Raymond, J. R.; Lohse, M. J.; Kobilka, B. K.; Caron, M. G.; Lefkowitz, R. J. The Genomic Clone G-21 Which Resembles a β -Adrenergic Receptor Sequence Encodes the 5-HT_{1A} Receptor. *Nature* **1988**, *335*, 358–360.
- (26) Pulito, V. L.; Li, X.; Varga, S. S.; Mulcahy, L. S.; Clark, K. S.; Halbert, S. A.; Reitz, A. B.; Murray, W. V.; Joliffe, L. K. An Investigation of the Uroselective Properties of Four Novel α_{1A} -Adrenergic Receptor Subtype-Selective Antagonists. *J. Pharmacol. Exp. Ther.* **2000**, *294*, 224–229.
- (27) Eltze, M.; Boer, R.; Sanders, K. H.; Kolossa, N. Vasodilatation Elicited by 5-HT_{1A} Receptor Agonists in Constant-Pressure-Perfused Rat Kidney Is Mediated by Blockade of α_{1A} -Adrenoceptors. *Eur. J. Pharmacol.* **1991**, *202*, 33–44.
- (28) (a) Ko, F. N.; Guh, J. H.; Yu, S. M.; Hou, Y. S.; Wu, Y. C.; Teng, C. M. (–)-Discretamine, a Selective α_{1D} -Adrenoceptor Antagonist, Isolated from *Fissistigma glaucescens*. *Br. J. Pharmacol.* **1994**, *112*, 1174–1180. (b) Buckner, S. A.; Oheim, K. W.; Morse, P. A.; Knepper, S. M.; Hancock, A. A. α_1 -Adrenoceptor-Induced Contractility in Rat Aorta Is Mediated by the α_{1D} Subtype. *Eur. J. Pharmacol.* **1996**, *297*, 241–248.
- (29) Melchiorre, C.; Bolognesi, M. L.; Budriesi, R.; Chiarini, A.; Giardinà, D.; Minarini, A.; Quaglia, W.; Leonardi, A. Search for selective antagonists at α_1 -adrenoceptors: neutral or negative antagonism? *Farmacol.* **1998**, *53*, 278–286.
- (30) (a) Noguera, M. A.; Ivorra, I. D.; D'Ocon, P. Functional evidence of inverse agonism in vascular smooth muscle. *Br. J. Pharmacol.* **1996**, *119*, 158–164. (b) Rossier, O.; Abuin, L.; Fanelli, F.; Leonardi, A.; Cotecchia, S. Inverse Agonism and Neutral Antagonism at α_{1A} - and α_{1B} -Adrenergic Receptor Subtypes. *Mol. Pharmacol.* **1999**, *56*, 858–866.
- (31) For a review, see Herbert, T. E.; Bouvier, M. Structural and Functional Aspects of G Protein-Coupled Receptor Oligomerization. *Biochem. Cell Biol.* **1998**, *76*, 1–11.
- (32) For example, see Zeng, F.-Y.; Wess, J. Molecular Aspects of Muscarinic Receptor Dimerization. *Neuropsychopharmacology* **2000**, *23*, S19–S29.
- (33) (a) Jones, K. A.; Borowsky, B.; Tamm, J. A.; Craig, D. A.; Durkin, M. M.; Dai, M.; Yao, W. J.; Johnson, M.; Gunwaldsen, C.; Huang, L. Y.; Tang, C.; Shen, Q.; Salon, J. A.; Morse, K.; Laz, T.; Smith, K. E.; Nagarathnam, D.; Noble, S. A.; Branchek, T. A.; Gerald, C. GABA_B Receptors Function as a Heteromeric Assembly of the Subunits GABA_BR1 and GABA_BR2. *Nature* **1998**, *396*, 674–679. (b) Kaupmann, K.; Malitschek, B.; Schuler, V.; Heid, J.; Froestl, W.; Beck, P.; Mosbacher, J.; Bischoff, S.; Kulik, A.; Shigemoto, R.; Karschin, A.; Bettler, B. GABA_B-Receptor Subtypes Assemble into Functional Heteromeric Complexes. *Nature* **1998**, *396*, 683–687. (c) Kuner, R.; Kohr, G.; Grunewald, S.; Eisenhardt, G.; Bach, A.; Kornau, H. C. Role of Heteromer Formation in GABA_B Receptor Function. *Science* **1999**, *283*, 74–77. (d) White, J. H.; Wise, A.; Main, M. J.; Green, A.; Fraser, N. J.; Disney, G. H.; Barnes, A. A.; Emson, P.; Foord, S. M.; Marshall, F. H. Heterodimerization Is Required for the Formation of a Functional GABA_B Receptor. *Nature* **1998**, *396*, 679–682.

- (34) Jordan, B. A.; Devi, L. A. G-Protein-Coupled Receptor Heterodimerization Modulates Receptor Function. *Nature* **1999**, *399*, 697–700.
- (35) Schertler, G. F.; Villa, C.; Henderson, R. Projection Structure of Rhodopsin. *Nature* **1993**, *362*, 770–772.
- (36) Unger, V. M.; Hargrave, P. A.; Baldwin, J. M.; Schertler, G. F. Arrangement of Rhodopsin Transmembrane α -Helices. *Nature* **1997**, *389*, 203–206.
- (37) Swindells, M. B.; Thornton, J. M. Modelling by Homolog. *Curr. Opin. Struct. Biol.* **1991**, *1*, 219–223.
- (38) Palczewski, K.; Kumasaka, T.; Hori, T.; Behnke, C. A.; Motoshima, H.; Fox, A. B.; Le Trong, I.; Teller, D. C.; Okada, T.; Stenkamp, R. E.; Yamamoto, M.; Miyano, M. Crystal Structure of Rhodopsin: a G Protein-Coupled Receptor. *Science* **2000**, *289*, 739–745.
- (39) Teller, D. C.; Okada, T.; Behnke, C. A.; Palczewski, K.; Stenkamp, R. E. Advances in Determination of a High-Resolution Three-Dimensional Structure of Rhodopsin, a Model of G-Protein-Coupled Receptors (GPCRs). *Biochemistry* **2001**, *40*, 7761–7772.
- (40) Kristiansen, K.; Dahl, S. G.; Edvardsen, O. A Database of Mutants and Effects of Site-Directed Mutagenesis Experiments on G Protein-Coupled Receptors. *Proteins* **1996**, *26*, 81–94.
- (41) Muller, G. Towards 3D Structures of G Protein-Coupled Receptors: a Multidisciplinary Approach. *Curr. Med. Chem.* **2000**, *7*, 861–888.
- (42) Carrieri, A.; Centeno, N. B.; Rodrigo, J.; Sanz, F.; Carotti, A. Theoretical Evidence of a Salt Bridge Disruption As the Initiating Process for the α_{1d} -Adrenergic Receptor Activation: a Molecular Dynamics and Docking Study. *Proteins* **2001**, *43*, 382–394.
- (43) Goodford, P. J. A Computational Procedure for Determining Energetically Favourable Binding Sites on Biologically Important Macromolecules. *J. Med. Chem.* **1985**, *28*, 849–857.
- (44) For a fully detailed description of this methodology, the reader is referred to the GRID manual available on line from the Internet at <http://www.moldiscovery.com>.
- (45) Chen, S.; Xu, M.; Lin, F.; Lee, D.; Riek, P.; Graham, R. M. Phe310 in Transmembrane VI of the α_{1b} -Adrenergic Receptor Is a Key Switch Residue Involved in Activation and Catecholamine Ring Aromatic Bonding. *J. Biol. Chem.* **1999**, *274*, 16320–16330.
- (46) Allen, F. H.; Kennard, O. 3D Search and Research Using the Cambridge Structural Database. *Chem. Des. Autom. News* **1993**, *8*, 31–37.
- (47) McMartin, C.; Bohacek, R. S. QXP: Powerful, Rapid Computer Algorithms for Structure-Based Drug Design. *J. Comput.-Aided Mol. Des.* **1997**, *11*, 333–344.
- (48) Carpy, A.; Colleter, J. C.; Leger, J. M. N-{2-(2,6-Dimethoxyphenoxy)ethyl}-1,4-benzodioxane-2-methylamine Hydrochloride (WB-4101). *Cryst. Struct. Commun.* **1981**, *10*, 1391–1395.
- (49) Cavalli, A.; Fanelli, F.; Taddei, C.; De Benedetti, P. G.; Cotecchia, S. Amino Acids of the α_{1b} -Adrenergic Receptor Involved in Agonist Binding: Differences in Docking Catecholamines to Receptor Subtypes. *FEBS Lett.* **1996**, *399*, 9–13.
- (50) Kraulis, P. J. MOLSCRIPT: A Program to Produce Both Detailed and Schematic Plots of Protein Structures. *J. App. Crystallogr.* **1991**, *24*, 946–950.
- (51) (a) Arunlakshana, O.; Schild, H. O. Some Quantitative Uses of Drug Antagonists. *Br. J. Pharmacol.* **1959**, *14*, 48–58. (b) Tallarida, R. J.; Cowan, A.; Adler, M. W. pA_2 and Receptor Differentiation: A Statistical Analysis of Competitive Antagonism. *Life Sci.* **1979**, *25*, 637–654. (c) van Rossum, J. M. Cumulative Dose–Response Curves. II. Techniques for the Making of Dose–Response Curves in Isolated Organs and the Evaluation of Drug Parameters. *Arch. Int. Pharmacodyn. Ther.* **1963**, *143*, 299–330.
- (52) De Lean, A.; Munson, P. J.; Rodbard, D. Simultaneous Analysis of Families of Sigmoidal Curves: Application to Bioassay, Radioligand Assay, and Physiological Dose–Response Curves. *Am. J. Physiol.* **1978**, *235*, E97–E102.
- (53) Cheng, Y. C.; Prusoff, W. H. Relationship Between the Inhibition Constant (K_i) and the Concentration of Inhibitor Which Causes 50% Inhibition (I_{50}) of an Enzymatic Reaction. *Biochem. Pharmacol.* **1973**, *22*, 3099–3108.

JM011066N